Viscoelastic Properties of Composite Tube Materials

by
Hwai-Jiang Jong
Prof. R. A. Schapery

Department of Aerospace Engineering and Engineering Mechanics
University of Texas at Austin

Final Project Report:
Interdisciplinary Design for Composite Coiled Tubulars: Effects of Visoelasticity
Under the MMS/OTRC Cooperative Research Agreement
1435-01-99-CA-31003
Task Order 16176
MMS Project Number 365

August 2001

OTRC Library Number: 08/01B114

For more information contact:

Offshore Technology Research Center
Texas A&M University
1200 Mariner Drive
College Station, Texas 77845-3400
(979) 845-6000

or

Offshore Technology Research Center
The University of Texas at Austin
1 University Station C3700
Austin, Texas 78712-0318
(512) 471-6989

A National Science Foundation Graduated Engineering Research Center

August, 2001

Viscoelastic Properties of Composite Tube Materials

Hwai-Jiang Jong
Prof. R. A. Schapery

Department of Aerospace Engineering and Engineering Mechanics
University of Texas at Austin

Abstract

In this study, an experimental approach to finding the linear viscoelastic properties of fiber wound composite tubes is presented. HYDRIL provided tubes of two different materials, which may be used in offshore applications; they are carbon and glass fiber reinforced epoxy in two types of layup (±45° and ±55°). A set of displacement ramp-to-failure tests was conducted on specimens cut from tubes to find the stress-strain curves and ultimate strengths of the four layups at room temperature. Methods of creep testing the entire tubes and rectangular coupon specimens cut from tubes for obtaining creep compliances of the materials are described. Master compliance curves for the ±55°carbon/epoxy and glass/epoxy are presented. The temperature shift factor has been found by testing the carbon/epoxy and glass/epoxy coupons at the temperatures 75°F, 103°F, 147°F, and 199°F. It is shown that the materials are thermorheologically simple, except for the need to include a temperature-dependent vertical shift factor.

1. Introduction

Fiber reinforced composite materials have been widely used in many structural applications. In this class of materials, if the underlying matrix is polymeric, then the material usually exhibits significant time-dependent mechanical behavior even at room temperature. When the long-term durability is of concern, good understanding of time-dependent behavior is needed.

The time-dependent mechanical behavior studied here comes from the composite material's intrinsic viscoelastic properties. Damage due to loading, and physical and chemical aging may also be significant, but these were not addressed in our experimental research. It is very important to understand these time-dependent phenomena through testing and analysis before the materials can be confidently employed in long-term, primary structural applications. Of all the durability concerns about the material, the linear viscoelastic properties play a fundamental role, as may be seen in a paper on damage growth [1] that was prepared as part of the research on this project. It was the purpose of this experimental study to obtain the linear viscoelastic properties of two materials that may be used in the offshore applications.

Section 2 describes the materials used in this study. The third section discusses the experimental approach to finding the viscoelastic properties. The testing results and data analysis are contained in section 4.

2. Material Description

The materials in this study were provided by Dr. Thomas Walsh, HYDRIL. They came in as four types of samples of 12-inch long circular cylindrical tubes. The tubes are made of ±45° or ±55° glass/epoxy and carbon/epoxy wound on an aliphatic polyketone liner to form the circular cylindrical shape. The same epoxy is used in the glass and carbon composite materials. Their stacking sequences, from inner to outer surfaces, and dimensions are in Table 1.

+/-45 glass/epoxy layup tube

Fiber angle/ply	Inner dia. (in)	Wall thick (in)	Outer dia. (in)
Liner	2	0.08	2.16
+45 glass	2.16	0.013	2.186
-45 glass	2.186	0.013	2.212
+45 glass	2.212	0.013	2.238
-45 glass	2.238	0.013	2.264
+45 glass	2.264	0.013	2.29
-45 glass	2.29	0.013	2.316
+45 glass	2.316	0.013	2.342
-45 glass	2.342	0.013	2.368

+/-55 glass/epoxy layup tube

Fiber angle/ply	Inner dia. (in)	Wall thick (in)	Outer dia. (in)
Liner	2	0.08	2.16
+55 glass	2.16	0.017	2.194
-55 glass	2.194	0.017	2.228
+55 glass	2.228	0.016	2.26
-55 glass	2.26	0.016	2.292
+55 glass	2.292	0.016	2.324
-55 glass	2.324	0.016	2.356
+55 glass	2.356	0.015	2.386
-55 glass	2.386	0.015	2.416

+/-45 carbon/epoxy layup tube

Fiber angle/ply	Inner dia. (in)	Wall thick (in)	Outer dia. (in)
Liner	2	0.08	2.16
+45 carbon	2.16	0.013	2.186
-45 carbon	2.186	0.013	2.212
+45 carbon	2.212	0.013	2.238
-45 carbon	2.238	0.013	2.264
+45 carbon	2.264	0.013	2.29
-45 carbon	2.29	0.013	2.316
+45 carbon	2.316	0.013	2.342
-45 carbon	2.342	0.013	2.368

+/-55 carbon/epoxy layup tube

Fiber angle/ply	Inner dia. (in)	Wall thick (in)	Outer dia. (in)
Liner	2	0.08	2.16
+55 carbon	2.16	0.016	2.192
-55 carbon	2.192	0.016	2.224
+55 carbon	2.224	0.016	2.256
-55 carbon	2.256	0.016	2.288
+55 carbon	2.288	0.016	2.32
-55 carbon	2.32	0.016	2.352
+55 carbon	2.352	0.015	2.382
-55 carbon	2.382	0.014	2.41

Table 1 Material configurations

3. Experimental Approach

The objective of this study was to acquire the materials' linear viscoelastic properties. A series of tests were conducted to acquire materials' data for subsequent analysis.

Ramp-to-Failure Tests

Firstly, displacement ramp-to-failure tests for the four lay-ups were conducted to obtain their ultimate strengths and stress-strain curves at room temperature. These tests were conducted on straight-sided coupons of their respective configurations. The coupons were cut from the tube along its generator line. They are therefore straight on two sides and are curved in the cross section. The liner was carefully removed, by grinding and peeling from the composites. All the coupons were one half inch wide and 9 inches long. Special curved tabs made of G10 fiber-woven glass/epoxy were machined to fit the cross-sectional curvature of the specimen. Because of this curvature, a width greater than one-half inch would not be conveniently used. For these relatively thick coupons, there may be free-edge effect in this creep and/or strength response, but this was not investigated.

Tube Creep Tests

Following the ramp-to-failure tests, 10% of ultimate strength at room temperature was chosen as the stress level in performing the linear viscoelastic creep tests on the entire tubes to obtain the creep compliances. The creep time selected was one hour, followed by a ten-hour recovery under no load. The stress level was chosen so that the viscoelastic properties are within linear range. The creep tests for tubes were all conducted at 75°F, because the tube could not fit in our high-temperature chamber. Liners 2" long each at the ends of the tubes were carefully machined off. Two circular cylindrical aluminum fittings, with diameter matching the tube's inner surface, were machined and bonded onto the liner-removed surfaces of the tube. Rods on the fittings were 2 inches long and 0.6 inch in diameter so as to fit the grip face of the INSTRON testing machine. The fitting was designed as a mechanism to transfer axial load from testing machine to the tube uniformly through the circumferential bond line. The design and assembly of the fitting and tube are shown in Fig. 1. Three rosette strain gages (Micro-Measurement's CEA-06-125UT-350) were bonded in the center section of the tube. They were positioned circumferentially at 120° with respect to each other to cancel any strain due to global bending of the tube.

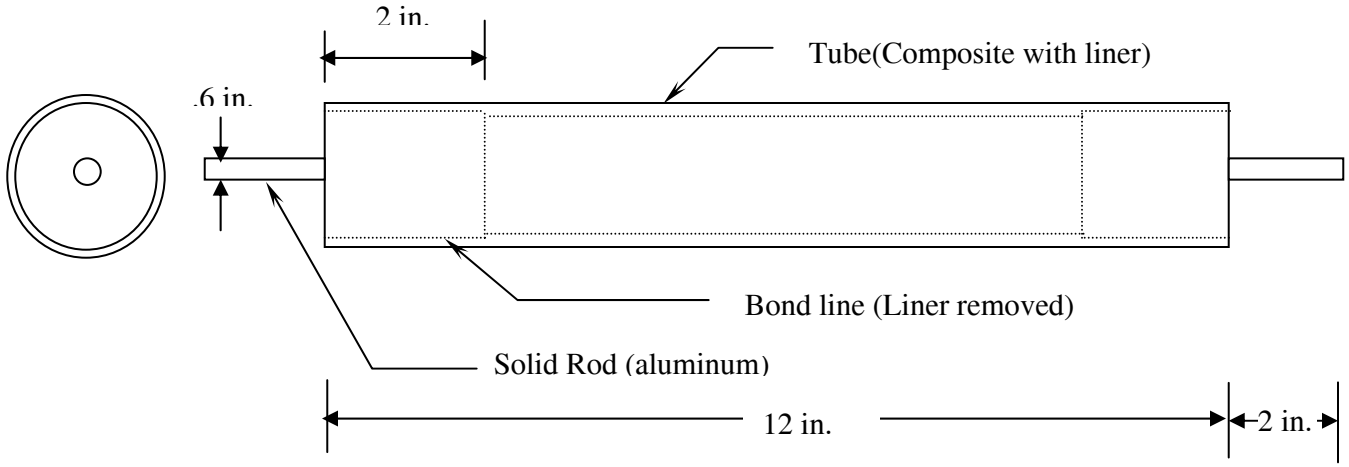

Fig. 1 Composite tube assembly

Since the tube was end-bonded to a solid aluminum fitting, when under uniaxial tensile loading its ends were prevented from free radial displacement due to the metal fitting's constraint. This situation caused a boundary effect that may propagate into the center area where the strains were to be measured. Therefore, depending on the structural geometry and the material's Poisson's ratio, the boundary layer effect may involve out-of-plane bending in the shell, which is undesirable because bending-free condition at the gage area is needed. In order to clarify this situation and validate the tube test approach to obtaining the creep compliance, a finite element model was constructed to analyze the linear elastic stresses and displacements around the strain gage area. The finite element model, coded in ABAQUS, was a circular cylindrical tube of an 8-layer ±45° carbon/epoxy angle ply layup, which was identical to some of the tubes in this study. The boundary conditions were prescribed by an axial displacement at one end of the tube, simulating the imposed crosshead displacement. This prescribed axial displacement resulted in a uniform axial strain of 1% at the gage section. Lamina linear elastic properties were provided by HYDRIL, which are shown in Table 2.

Material	E_{11} (msi)	E_{22} (msi)	ν_{12}	G_{12} (msi)	G_{23} (msi)
Carbon/Epoxy	21.46	1.399	.3	.6597	.6597
Glass/Epoxy	6.53	1.88	.28	.85	.5
Liner	.15	.15	.4	.0536	.0536

Table 2 Material properties in principal material directions provided by HYDRIL

The radial displacement, which is directly indicative of the boundary bending effect, is shown in Fig. 2. It is demonstrated that the middle area of the tube does not show any significant axial bending deformation due to the ends. For comparison purposes, a separate condition in which the tube is under uniform internal pressure was also analyzed using the same ABAQUS model (Fig. 3). In the pressurized condition, a well-established analytical result is available [2], in which the tube is isotropic (aluminum is chosen in this study), is included to compare to the model. The results are shown in Fig. 4. It is seen that the boundary layer effect propagates into the interior section of the tube for both the composite and isotropic cases. The isotropic result of the finite element model fits the analytical solution very well. It is interesting to note that even though the composite has a relatively high Poisson's ratio compared to aluminum, the boundary effect does not propagate into the center part in axially loaded condition as far as it does in the pressurized condition. Therefore, it is verified that when the tube is under a uniform axial boundary condition (load or displacement), the boundary effect can be neglected in our tests. Furthermore, by classical lamination theory [3], if the liner is neglected and the layup is antisymmetric and angle-ply, as our ±45° composites, the inplane axial and shear strains are uncoupled, and the tube is under a uniaxial stress conditions just as the straight coupon.

Temperature Shift Factor Tests

Straight-sided coupons of two lay-ups, ±55° carbon/epoxy and ±55° glass/epoxy were cut out from tubes for creep tests at constant temperatures of 75°F, 103°F, 147°F, and 199°F. The purpose of this set of tests was to find the temperature shift factor a_T, provided that the matrix is thermorheologically simple [4]. The two types of materials were both tested at the same conditions, except that ±55° carbon/epoxy wasn't tested at 199°F. They served as a check that the resulting shift factor is the same for an epoxy reinforced with either glass or carbon fibers.

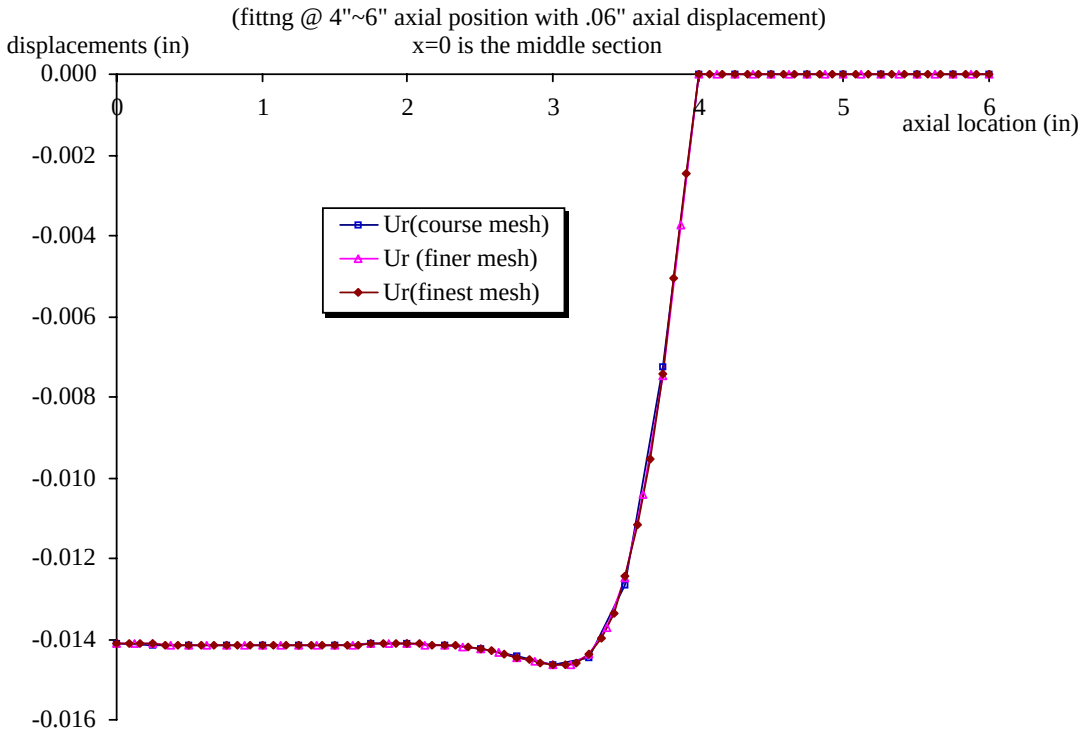

Fig. 2 The radial displacement of composite tube under uniaxial tensile boundary condition

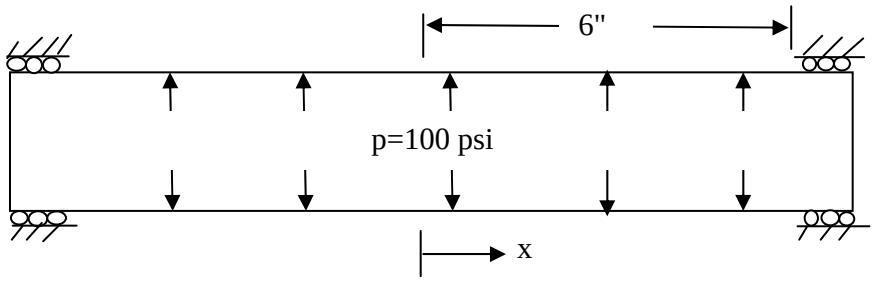

Fig. 3 Tube under uniform internal pressure

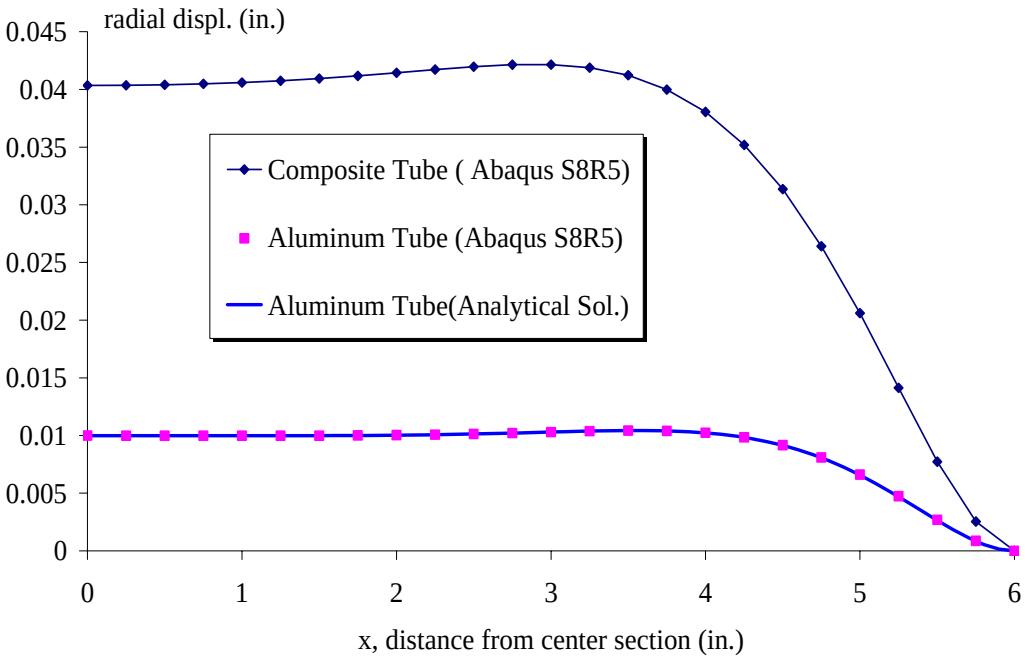

Fig.4 Radial Displacements of Circular Cylindrical Tube
under Uniform Internal Pressure

4. Test Results and Data Analysis

4.1. Coupon Ultimate and Tube Creep Compliance Tests

The ultimate strength test results for the four layups can be seen in Table 3, where the data are the average from two replica coupons for each material. The stress-strain curves for all materials are shown in Figs.5&6. The creep compliances from tube tests are also shown in Table 3. The unit of time is second. Note that the tubes were tested only under creep condition at 10% ultimate stress level. The data from the coupon tests can be used directly to calculate Young's modulus and Poisson ratio, as is normally done in all flat coupon tests. However, the creep compliances of the four layups from the tube tests are more involved. Since the cross section at the gage area on the tubes is comprised of a layer of liner and 8 layers of fiber composites, certain modification is required for calculating the creep compliance of the composite in the absence of liner material. Assumptions made in this calculation are that the quasi-elastic condition applies [5] and the rule of mixtures can be used [3]. Under these assumptions, the creep compliance can be easily backed out from the tubes' creep data if the creep compliance of the liner and the tubes' cross sectional geometries are known. The axial loading on the tube is F(t), the cross sectional area and the creep compliance of the composite and liner are A_c,$D_c(t)$, and A_l,$D_l(t)$ respectively. By force equilibrium,

$$F(t) = \left(\frac{A_c}{D_c(t)} + \frac{A_l}{D_l(t)} \right) \varepsilon(t) \tag{1}$$

where $\varepsilon(t)$ is the acquired axial strain data on the tube. The compliance of the composite D_c can be calculated from

$$D_c(t) = \frac{A_c}{\frac{F(t)}{\varepsilon(t)} - \frac{A_l}{D_l(t)}} \tag{2}$$

The calculated D_c was curve fitted, with D_c plotted against time raised to an exponent n, whichever gives the straightest line on the plot. The D_c is then given in the form of a power law as

$$D_c(t) = D_0 + D_1 t^n. \tag{3}$$

The values of D_0,$D_1$and n are listed in Table 3, and t is in seconds. Note that same exponents were found for both carbon and glass composites. This is to be expected because the same epoxy is used and the matrix is soft relative to the fibers.

Material	±45° Carbon		±55° Carbon		±45° Glass		±55° Glass		Liner
Specimen Type	Coupon	Tube	Coupon	Tube	Coupon	Tube	Coupon	Tube	Coupon
E(msi)	2.559	2.506*	1.675	1.667*	2.272	1.832*	1.806	1.721*	
Poisson ratio	0.774	0.755	0.504	0.468	0.451	0.477	0.305	0.36	0.43
UTS(ksi)	14.882		9.481		10.11		7.84		
Do(msi^{-1})		0.399		0.6		0.546		0.581	3.655
D1($msi^{-1}sec^{-n}$)		0.0055		0.0046		0.0045		0.0042	0.193
n		0.23		0.23		0.23		0.23	0.215

* Calculated from the inverse of D_0

Table 3 Results for creep tests on tubes and strength(UTS) tests on straight coupons at 75°F

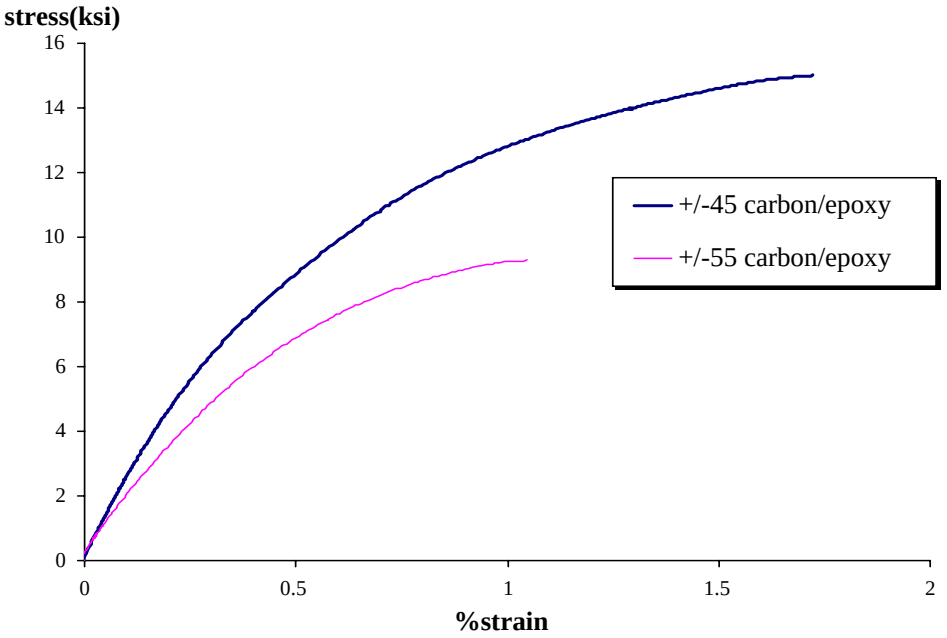

Fig. 5 ±45° and ±55° carbon/epoxy ramp test results

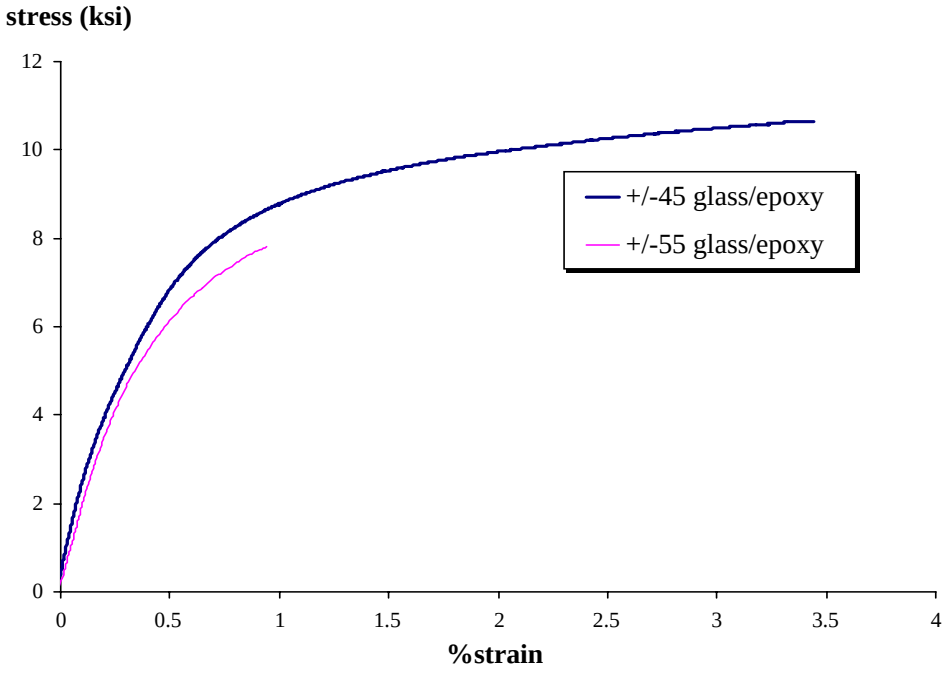

Fig. 6 ±45° and ±55° glass/epoxy ramp test results

4.2. Temperature Shift Factor a_T and the Master Curve

The temperature shift factors a_T were found by creeping the sample (under constant load) for 1 hour and recovering (following load removal) for 10 hours, at 4 temperature levels. The sample here refers to the straight coupon, as our environmental chamber could only accommodate short coupons for elevated temperature conditions. Several cycles were performed until the creep curves did not show significant cycle-to-cycle deviation. For comparison purposes, two types of layups were used to check the consistency of the data for calculating a_T. Fig. 7 and Fig.8 are the master curves for the ±55° carbon /epoxy and ±55° glass/epoxy coupons respectively. Both graphs show a master creep compliance curve with master reference temperature at T_M=103°F. The master creep compliance can be expressed as Eq. 3, where t is replaced by reduced time ξ, with D_0=0.502 msi^{-1}, D_1=0.009 1/msi/sec^n, for carbon/epoxy, and D_0=0.466 msi^{-1}, D_1=0.0073 1/msi/sec^n for glass/epoxy. The exponent n, which is 0.23, is the same for both materials, as noted above.

The shifting factor agrees with the Arrhenius equation, as can be seen in Fig. 9. The thermal activation energy was calculated by fitting the line to Arrhenius equation as follows,

$$\log a_T = \frac{\Delta F}{2.303R}\left(\frac{1}{T} - \frac{1}{T_M}\right) \tag{5}$$

where, ΔF is the thermal activation energy, R is the perfect gas constant and is 1.99 cal/mole-°K. Equating the slope of the line to the coefficient, the thermal activation energy is calculated as

$$\Delta F = 5342.3 \times 2.303 \times R = 24.5 \qquad Kcal/mole \tag{6}$$

which is a typical value for epoxy.

The master curves also required vertical shift ΔD on a linear scale, as shown in Fig. 10, which indicates the effect of temperature on D_0. The need for vertical shift was expected for material at temperature below the glass transition point [5].

During the course of creep tests, viscoplastic nonrecoverable strains for the time scale studied were observed at the end of the recovery period for all cycles. The plastic strain, although existing, decreases from cycle to cycle. Figs.11&12 show the accumulated viscoplastic strain of the ±55° glass and carbon coupon during the cycles.

In order to find if the room temperature creep properties evolve with high temperature history, room temperature creep tests were performed following high temperatures creep at 103°F and 199°F. The results are plotted in Fig. 13 with the very original room temperature creep data. It is seen that the creep compliance at room temperature does change due to prior thermal history. What is interesting is that the compliance tends to increase with prior temperature history, which seems to indicate there is possibly damage induced softening due to previous loading, rather than significant post-cure hardening.

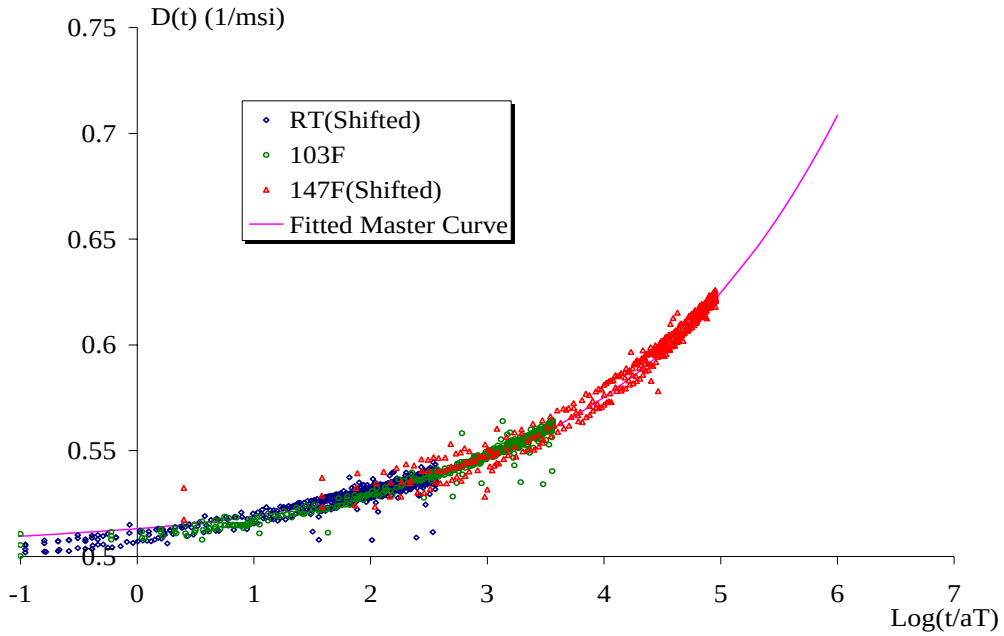

Fig. 7 Master creep compliance curve of +/-55 carbon/epoxy at 103F

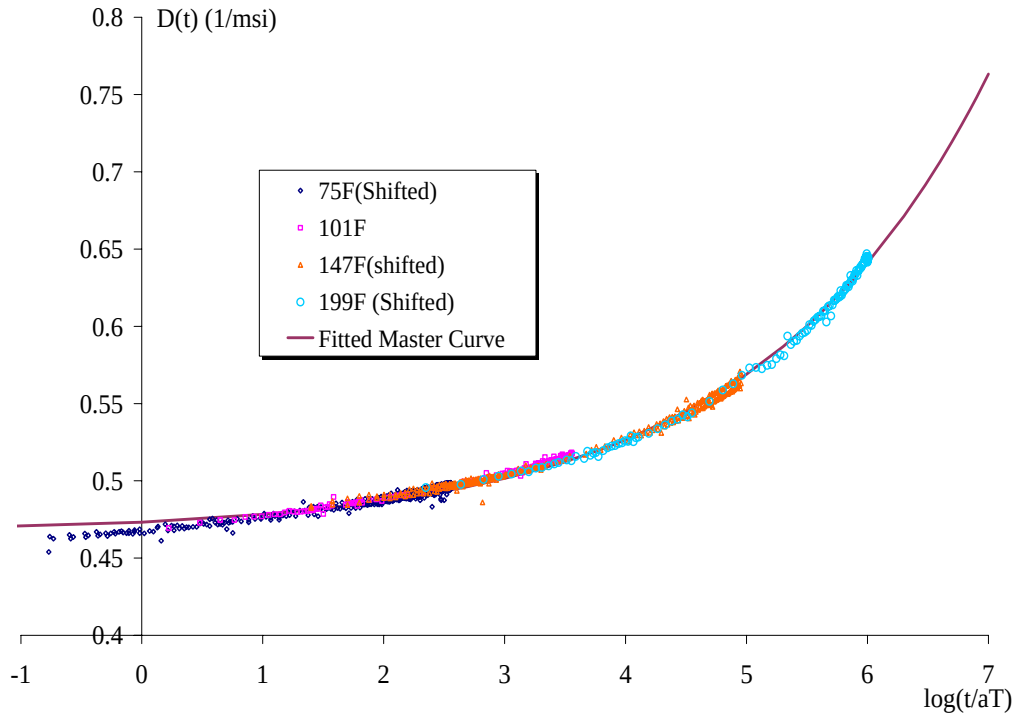

Fig. 8 Master creep compliance curve of +/- 55 glass/epoxy at 103F

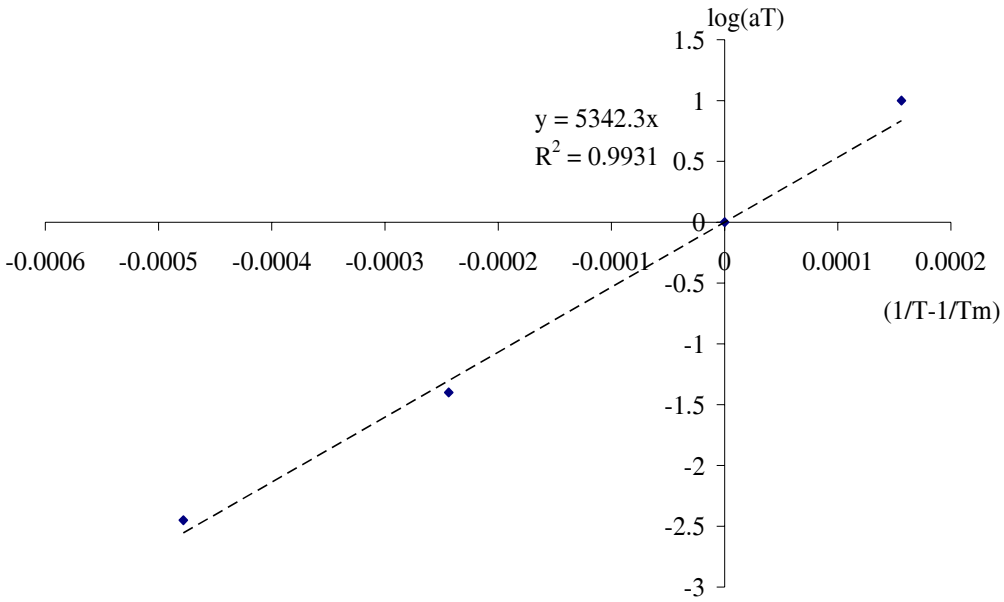

Fig. 9 Temperature shift factor

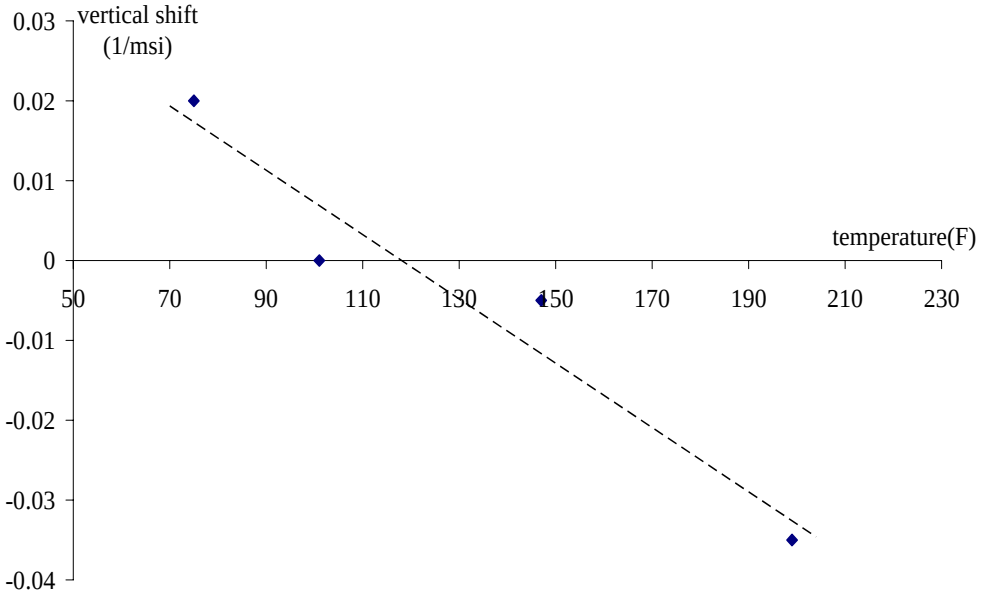

Fig. 10 Vertical Shift in D(t) for +/-55 glass/epoxy

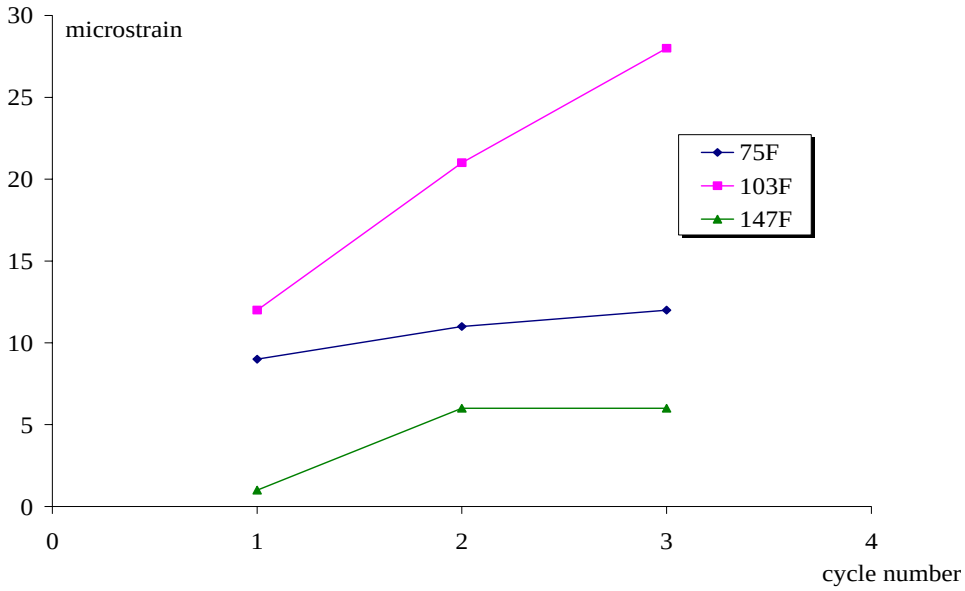

Fig. 11 Accumulated viscoplastic strains (+/- 55 Carbon)

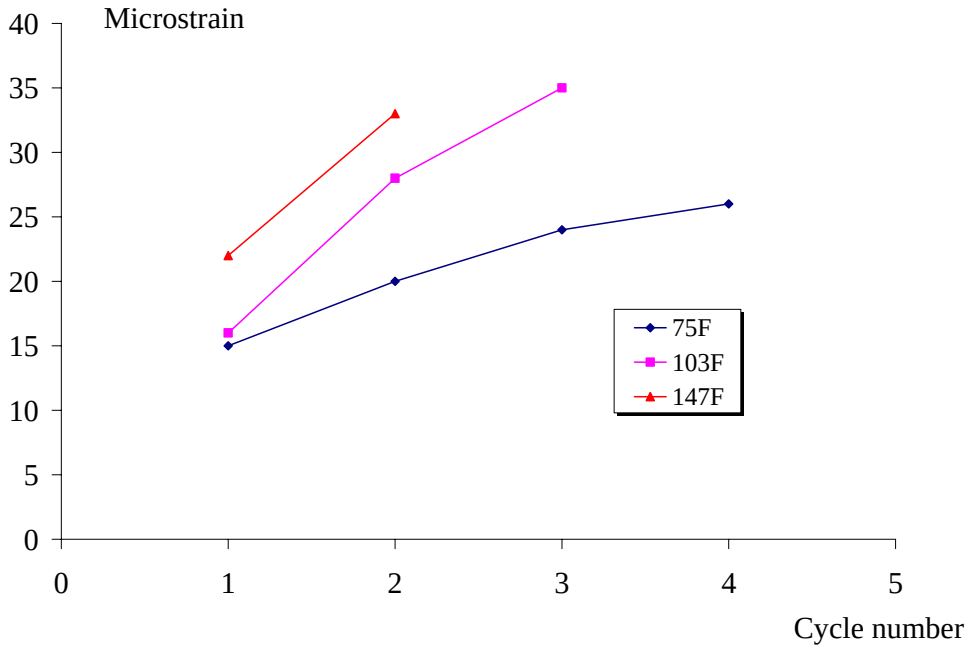

Fig.12 Accumulated viscoplastic strains (+/- 55 glass)

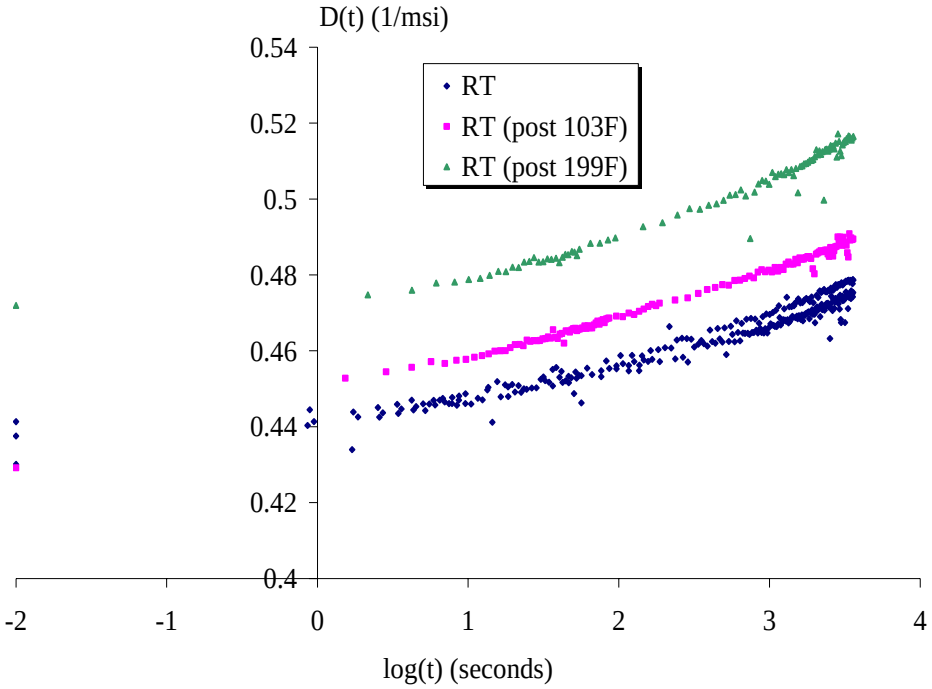

Fig. 13 Comparison of RT Creep tests at different stages

4.3 Ply-level Properties in Material Coordinates

It is of interest to find the ply-level material properties E_{11}, E_{22}, ν_{12}, G_{12} in their principal directions. By using the acquired creep data of the tubes, it is possible to back-out these properties by classical lamination theory, with suitable boundary conditions on the shells of the tubes. Based on analysis on the material's sensitivity to properties E_{11}, E_{22}, G_{12}, and ν_{12}, their values as functions of time can be calculated iteratively using Newton's method. As for the materials in this study, in which the ply-angle is ±45° or ±55°, it was found from sensitivity analysis in this study that the laminate is most sensitive to E_{22} and G_{12}, as expected. However, an accurate estimate of E_{11} and ν_{12} is also required in order to yield a good match to the measured laminate's strains; some of the data supplied data in Table 2 did not seem to correlate well with our results, and thus values in Table 2 were not used. Due to unavailability of the necessary specimens, these calculations were not carried out in this study.

5. Conclusions

The creep compliance data for the carbon and glass fiber/epoxy used in the composite tubes have been obtained. Time-temperature shifting using horizontal log scale and vertical linear scale was employed to construct the master creep compliance curves for ±55°carbon /epoxy and ±55° glass/epoxy composites, respectively. The collapsed creep curves have shown that the composites in this study are thermorheologically simple apart from the need for vertical shifting; the long term compliance can be obtained in the same manner for ±45° carbon/epoxy and ±45° glass/epoxy. The thermal activation energy of 24.5Kcal/mol was calculated from the Arrhenius equation. In all cases, for tubes and coupons the creep compliances were found to obey the power law in Eq.(3) with an exponent of 0.23. That the same values of activation energy and exponent were found for carbon and glass fiber composites is consistent with the fact that the underlying matrix material is the same for all layup configurations.

References

1. R. A. Schapery “Homogenized Constitutive Equations for Linear Viscoelastic Unidirectional Composites with Growing Transverse Cracks” Mechanics of Time Dependent Materials, in press
2. S. Timoshenko, “Theory of Plates and Shells” McGraw Hill, 2nd Ed.., pp.471-478 (1959)
3. R. F. Gibson “Principle of Composite Material Mechanics” McGraw Hill (1994)
4. J. D. Ferry “Viscoelastic Properties of Polymers” John Wiley & Sons (1980).
5. R. A. Schapery “Viscoelastic Behavior and Analysis of Composite Materials” in L. J. Broutman and R.H.Krock (ed.),Composite Materials, Vol. 2 Mechanics of Composite Materials, Chap. 4, Academic Press (1974)

Acknowledgement

This research was sponsored by the Mineral Management Services and grants from industry through the Offshore Technology Research Center.